Supplementary Information

High-Resolution Structures and Orientations of Antimicrobial Peptides Piscidin 1 and Piscidin 3 in Fluid Bilayers Reveal Tilting, Kinking, and Bilayer Immersion

B. Scott Perrin Jr., Ye Tian, Riqiang Fu, Christopher V. Grant, Eduard Y. Chekmenev, William E. Wieczorek, Alexander E. Dao, Robert M. Hayden, Caitlin M. Burzynski, Richard M. Venable, Mukesh Sharma, Stanley J. Opella, Richard W. Pastor, and Myriam L. Cotten*

*To whom correspondence should be addressed: Myriam L. Cotten, Department of Chemistry, Hamilton College, Clinton NY, USA, Tel.: (315) 859-4243; Fax: (315) 859-4807;

E-mail: **mcotten@hamilton.edu**

Circular Dichroism Experiments

To obtain 3:1 DMPC/DMPG and 1:1 POPE/POPG lipid mixtures, appropriate amounts of lipids dissolved in chloroform were added to round bottom flasks. The solvent was evaporated under nitrogen gas prior to overnight lyophilization to remove any residual organic solvent. A 5 mM stock solution of lipids was obtained by adding phosphate buffer (10 mM potassium phosphate, 0.1 mM EDTA, pH 7.4) to each lipid film and performing five freeze thaw cycles to homogenize the mixture. Extrusion was carried out using an Avanti Polar Lipid Mini Extruder fitted with 100-nm filters. Eleven passes were carried out to obtain ~100-nm diameter Large Unilamellar Vesicles (LUV). The lipid vesicles were mixed with the peptide to obtain a peptide-to-lipid ratio of 1:60 and a peptide concentration of 50 μM. CD spectra were acquired on a Jasco 815 instrument from 260 to 190 nm using a resolution of 0.1 nm, sensitivity of 100 millidegrees, bandwidth of 1.0 nm, response of 8 s, and scan speed of 20 nm/min over

four accumulations. Background spectra obtained from samples containing lipid vesicles alone were subtracted from the spectra acquired for the peptide-lipid mixtures. The mean residue ellipticity was calculated using exact peptide concentrations determined by amino acid analysis performed at the Keck Biotechnology Resource Laboratory (Yale University, New Haven, CT). The percent helical content was obtained using the mean residue ellipticity of the peptide at 222 nm and the method described by Yang *et al.*[1]

^{15}N Solid-state NMR Experiments for Structural Work

HETCOR and de-HETCOR spectra were obtained using previously reported parameters[2] that are summarized here. For each spectrum, a recycle delay of 4 s and 32-48 t_1 increments with 192-512 transients each were used. During data acquisition, temperature settings were 40±0.1 and 32±0.1 ºC for 3:1 DMPC/DMPG and 1:1 POPE/POPG, respectively. A proton RF amplitude of 62.5 kHz was applied during MSHOT proton homonuclear decoupling in the t_1 dimension (proton detection) and during SPINAL decoupling in the t_2 dimension (^{15}N detection). A dwell time of 54.0 μs in the proton chemical shift dimension was obtained by setting the delay τ_d to 7.0 μs. The proton carrier frequency was centered on the proton chemical shift dimension for the amide protons of piscidin. Spectra did not display any artifacts due to quadrature detection. An experimentally-determined scaling factor of 0.32 that is somewhat smaller than the theoretical value of 0.35 was applied to the scale in the t_1 dimension. For the deHETCOR spectra, no ^{15}N RF pulses were applied during the proton chemical shift evolution in the t_1 dimension. In contrast, the HETCOR spectra were collected using an ^{15}N RF amplitude of 45 kHz in the t_1 dimension to cancel out the ^{1}H-^{15}N dipolar couplings. To transfer the magnetization from the amide protons to their closest ^{15}N spins, a WIM-12 (*w*indowless *i*sotropic *m*ixing) sequence was applied using ^{1}H and ^{15}N RF amplitudes of 48 kHz and a short mixing time of 124.8 μs to ensure that every ^{15}N signal

from multiply ^{15}N-labeled piscidin could be detected.

Resonance Assignments

As explained in the main text, to ensure that correct assignments were made when multiply labeled samples were analyzed, assignments of p1 in 3:1 DMPC/DMPG were done with a large number of singly-labeled peptides (H3, H4, F6, R7, V10, V12, K14, H17, R18, V20). In the triply-labeled peptide F2I5G8, the assignment of F2 to the signal associated with a relatively low D_{NH} (equivalent to 2DC) and a high CS of 72.8 ppm was made knowing that helical fraying at the amino end could yield NMR restraints outside the range expected for in-plane α-helices. Therefore, there were two possible permutations left for assigning I5 and G8 to D_{NH} values of 8.7 and 7.4 kHz. Due to the periodicity of the wave every 3.6 in an α-helix, H4 and G8 were expected to be on the same side of the sinusoid. Since H4 (7.9 kHz) is on the side of the sinusoid with smaller D_{NH} values, G8 was assigned to the 7.4 kHz splitting and I5 to the remaining D_{NH} (8.7 kHz). L19 was run in a doubly-labeled peptide L19V20 but V20 had been run in a singly peptide giving a D_{NH} of 9.4 kHz, therefore L19 was assigned to the D_{NH} at 5.3 kHz. I9 and T15 yielded D_{NH} of 9.7 and 5.8 kHz. Since T15 and L19 are almost one helical turn apart, there were expected to yield similar D_{NH}, allowing us to assign T15 and I9 to the splittings of 5.8 and 9.7 kHz, respectively. In V10G13I16, V10 was run as a singly labeled peptide producing a D_{NH} of 9.0 kHz, hence D_{NH} values of 8.3 and 10.2 kHz were left for G13 and I16. Since I16 and V20 are approximately one helical turn apart and V20 has a D_{NH} of 9.4 kHz, I16 was confidently assigned to the splitting of 10.2 kHz and G13 to that of 8.3 kHz. Finally, T21 and G22 were run in a doubly-labeled peptide. The dipolar coupling (2 kHz) and chemical shift (131.4 ppm) of one residue were outside of the range expected for an ordered helix, therefore they were assigned to the last residue of the helix, G22, while T21 was assigned to the splitting of 9.2 kHz, very close to that of H17 (9.8 kHz), four residues

away. As a result of this logical process, ^{15}N CS and D_{NH} values were assigned without ambiguity for p1 in PC/PG. Because D_{NH} and CS values collected for the other peptides were similar to those of p1 in PC/PG, its assignments were used to guide those for the other peptides. Table S2 summarizes the complete assignments for the two peptides in the two lipid systems. As expected for peptides lying (almost) perpendicular to the bilayer normal, the resonances are polarized[3]. This means that the residues at the interface between polar and nonpolar sides of the amphipathic helix have smaller dipolar couplings than residues in the center of the polar and nonpolar faces. For instance, I9 and R7 in the center of the nonpolar and polar face of p1 in PC/PG, respectively, have large dipolar couplings of 9.7 and 9.9 kHz, respectively. In contrast, V12 and G8 near the boundary between polar/nonpolar residues have D_{NH} of 6.9 and 7.4 kHz, respectively. The pattern is similar in p3, with R7 and I9 having the largest D_{NH} in PC/PG. In PE/PG, again the largest D_{NH}'s in p1 are for R7 (10.1 kHz) and I9 (9.5 kHz). In this lipid system, the largest D_{NH} on the polar side belongs to H11 (10.5 kHz) rather than R7 (9.6 kHz). On the nonpolar side of p3 in PE/PG, both I5 and I9 have large D_{NH} of 9.5 and 9.6 kHz, respectively.

Dipolar and Chemical Shift Wave Analysis

The ^{15}N-^{1}H dipolar coupling, DC, for the peptide backbone was calculated from the refined NMR and MD structures as

$$\mathrm{DC} = D_a\left(\frac{3\cos^2(\theta)-1}{2}\right) = \frac{1}{2}\left|D_{\mathrm{NH}}\right| \qquad (1)$$

where D_a is the axial component of the alignment tensor, and θ is the angle of the NH vector with respect to the bilayer normal (Fig. S1). DC is calculated from the measured dipolar splitting (D_{NH}) in the de-HECTOR NMR spectra. As Opella and coworkers have previously described,[4] DC restraints for an α-helix form a sinusoidal pattern (or dipolar wave) when plotted against residue number (starting from the first amide group). The amplitude and phase of the wave peaks are determined by the tilt angle τ and

azimuthal rotation angle ρ of the helix, respectively. A D_a value of 10.735 kHz was used to calculate ^{15}N-^{1}H DC. The ^{15}N CSA restraints for the refined NMR and MD structures were calculated using the NMR facility in CHARMM with the well-established ^{15}N chemical shift tensor amplitudes of σ_{11} = 37 ppm, σ_{22} = 50 ppm, and σ_{33} = 190 ppm for all non-glycine residues and σ_{11} = 14 ppm, σ_{22} = 37 ppm, and σ_{33} = 183 ppm for glycine residues[5]. The experimental ^{15}N CSA values were also fitted to CS waves. The DC and CS wave analysis, which used Levenberg-Marquardt minimization,[6-8] revealed a kink in the (y,z) plane (Fig. 1B) at residue 13, so τ and ρ were calculated separately for residues 3 to 10 and 14 to 20, and their respective differences were named $\Delta\tau$ ($\tau_N - \tau_C$) and $\Delta\rho$ ($\rho_N - \rho_C$) where the subscripts N and C denote the N- and C-ends, respectively. For p3 in PE/PG, waves were fitted to residues 4 to 10 due to the lack of experimental DC for position 3. The peptides did not exhibit kinking in the plane of the membrane surface.

Statistical Analysis

This subsection describes the statistical analysis used for the refined NMR structures (NMRr) and MD simulations.

Refined NMR Structures−For each peptide/lipid system, values of τ, ρ, $\Delta\tau$, and $\Delta\rho$ were obtained from each of the 10 lowest energy peptide structures, and the standard deviation σ calculated to estimate the uncertainty.

MD Simulations−Block sizes of 10 ns yielded independent estimates of τ, ρ, and depth of insertion. The uncertainty in these quantities is determined by the standard errors in the mean (se), which was obtained by dividing the standard deviations of the averages from each block by the square root for the number of blocks (9 blocks in this case). The se for a quantity A is denoted se[A] or uncertainty in A. To a good approximation, if two means differ by more than twice their standard errors, it can be

inferred that they are not statistically equivalent. Root mean squared fluctuations (rmsf) were obtained as the standard deviations of the instantaneous values of the simulated quantity over the last 90 ns of each trajectory (i.e., the rmsf is the "width" of the distribution).

Table S1: Percent helical content as determined from CD at 21 °C for p1 and p3 in the presence of different vesicles at a 1:60 peptide-to-lipid ratio.

pH 7.4 **% helical content**	3:1 POPC/POPG	1:1 POPE/POPG	3:1 DMPC/DMPG
P1	98	95	99
P3	93	93	100

pH 6.0 **% helical content**	3:1 POPC/POPG	1:1 POPE/POPG	3:1 DMPC/DMPG
P1	91	81	91
P3	84	73	85

Table S2: Experimental solid-state NMR data. The sign of the dipolar splittings (D_{NH}) was established as described by Bertram *et al.*[9]

Residue Number	p1 in 3:1 DMPC/DMPG		p1 in 1:1 POPE/POPG	
	^{15}N Chemical Shift (ppm)*	Dipolar Splitting (kHz)	^{15}N Chemical Shift (ppm)*	Dipolar Splitting (kHz)
F1	20	Not detected	None detected	None detected
F2	72.9	-5.8	76.5	-5.2
H3	50.0	-8.2	58.4	-8.4
H4	61.9	-7.9	63.5	-7.6
I5	49.6	-8.7	47.5	-9.2
F6	63.7	-8.5	65.7	-8.4
R7	50.7	-9.9	50.1	-10.1
G8	45.6	-7.4	47.1	-6.3
I9	57.3	-9.7	53.2	-9.5
V10	54.0	-9.0	56.0	-9.5
H11	63.1	-10.0	70.4	-9.1
V12	47.6	-6.9	49.4	-8.1
G13	43.7	-8.3	44.8	-8.6
K14	56.7	-9.8	61.0	-10.8
T15	66.6	-5.8	68.9	-5.7
I16	39.9	-10.2	40.4	-10.1
H17	58.6	-9.8	61.1	-9.6
R18	65.6	-9.5	59.3	-10.2
L19	53.6	-5.3	52.6	-6.2
V20	48.4	-9.4	47.1	-9.7
T21	47.8	-9.2	50.2	-9.2
G22	131.4	2.0	123	None detected

Residue Number	p3 in 3:1 DMPC/DMPG		p3 in 1:1 POPE/POPG	
	^{15}N Chemical Shift (ppm)*	Dipolar Splitting (kHz)	^{15}N Chemical Shift (ppm)*	Dipolar Splitting (kHz)
F1	None detected	None detected	None detected	None detected
I2	54.7	None detected	82.0	None detected
H3	59.0	-5.8	62.5	None detected
H4	65.3	-7.2	71.5	-6.3
I5	45.9	-9.2	51.3	-9.5
F6	67.3	-7.8	67.4	-7.4
R7	37.5	-9.9	41.5	-9.6
G8	44.1	-7.7	47.1	-7.9
I9	55.6	-9.5	51.8	-9.6
V10	44.6	-8.9	44.2	-9.6
H11	57.2	-9.7	61.5	-10.5
A12	55.6	-7.6	51.4	-7.8
G13	55.4	-8.7	54.6	-8.9
R14	49.2	-9.2	50.3	-10.0
S15	62.8	-8.3	65.6	-7.8
I16	38.0	-9.9	36.5	-10.1
G17	45.1	-9.5	41.8	-9.9
R18	54.5	-9.8	57.8	-9.8
F19	63.2	-5.7	58.6	-7.4
L20	49.1	-9.3	50.0	-10.2
T21	43.8	-7.0	41.1	-8.0
G22	44.6	-7.0	39.0	-7.7

* With respect to $(NH_4)_2SO_4$ solution.

Table S3. Comparison of τ, ρ, and depth calculated from MD simulations for p1 and p3 in 3:1 DMPC/DMPG. The rmsf for MD structures are shown in parentheses.

Peptide	Charged Histidines	Residues 3 to 10			Residues 14 to 20		
		τ_N (°)	ρ_N (°)	Depth (Å)	τ_C (°)	ρ_C (°)	Depth (Å)
p1 PC/PG	None	91 (7)	265 (11)	3.4 (0.1)	87 (9)	245 (13)	3.3 (0.1)
p1 PC/PG	3, 4, 11	90 (7)	254 (12)	3.0 (1.0)	89 (8)	231 (14)	3.1 (0.9)
p1 PC/PG	3, 4, 11, 17	85 (6)	263 (12)	1.9 (0.9)	82 (7)	246 (11)	0.2 (0.9)
p3 PC/PG	None	93 (7)	245 (11)	3.7 (0.1)	85 (8)	225 (11)	3.4 (0.1)
p3 PC/PG	3, 4, 11	96 (6)	251 (10)	2.7 (0.7)	93 (8)	231 (11)	4.0 (0.7)
p1 PE/PG	None	92 (8)	256 (13)	1.0 (0.1)	90 (9)	236 (12)	1.4 (0.1)
p3 PE/PG	None	93 (7)	241 (11)	2.4 (0.1)	86 (8)	223 (10)	2.3 (0.1)
Average Fluctuation		7	11	0.9	8	12	0.9

* Standard errors in τ (se[τ]) and rmsf[τ] are 2° and 1°; respectively. se[ρ] and rmsf[ρ] are 3° and 1°; respectively. se[depth] and rmsf[depth] are 0.3 Å and 0.01 Å; respectively.

Table S4: NMR restraints as a function of pH at both extremities of piscidin 1 in 3:1 DMPC/DMPG bilayers.

	^{15}N chemical shifts (ppm)		**^{15}N/^{1}H dipolar couplings (kHz)**	
Residue	pH 6	pH 8.8	pH 6	pH 8.8
F2	72.9	53.6	5.8	0
I5	49.6	45.1	8.7	11.2
G8	45.6	45.3	7.4	7.4
L19	53.6	56.0	5.3	4.8
V20	48.4	46.0	9.4	9.6

Table S5. NMR restraints and structure statistics

Average pairwise RMSD (Å) for Backbone Atoms (C, CA, N, O)

	From the lowest energy structure	From the average structure
Piscidin 1 in 3:1 DMPC/DMPG:		
Residues 1 to 22:	0.632	0.556
Residues 3 to 20:	0.483	0.390
Residues 3 to 10:	0.497	0.375
Residues 14 to 20:	0.414	0.351
Piscidin 3 in 3:1 DMPC/DMPG:		
Residues 1 to 22:	0.724	0.590
Residues 3 to 20:	0.541	0.386
Residues 3 to 10:	0.414	0.276
Residues 14 to 20:	0.598	0.450
Piscidin 1 in 1:1 POPE/POPG:		
Residues 1 to 22:	0.590	0.535
Residues 3 to 20:	0.432	0.366
Residues 3 to 10:	0.424	0.363
Residues 14 to 20:	0.397	0.312
Piscidin 3 in 1:1 POPE/POPG:		
Residues 1 to 22:	0.616	0.569
Residues 3 to 20:	0.423	0.355
Residues 3 to 10:	0.302	0.235
Residues 14 to 20:	0.474	0.433

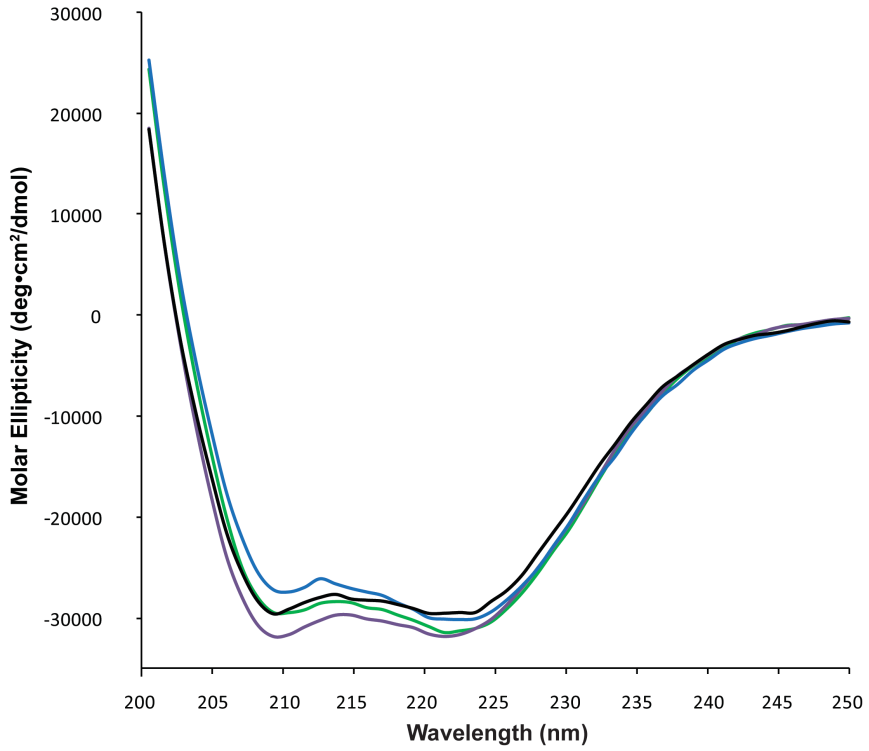

Figure S1. CD spectra for p1 and p3 in the presence of 3:1 DMPC/DMPG and 1:1 POPE/POPG. The peptide-to-lipid ratio was 1:80. Data collected in DMPC/DMPG are shown in green (p1) and purple (p3) while data obtained in 1:1 POPE/POPG are displayed in blue (p1) and black (p3). The data were recorded at 21 °C in phosphate buffer (10 mM potassium phosphate, 0.1 mM EDTA, pH 7.4).

A-

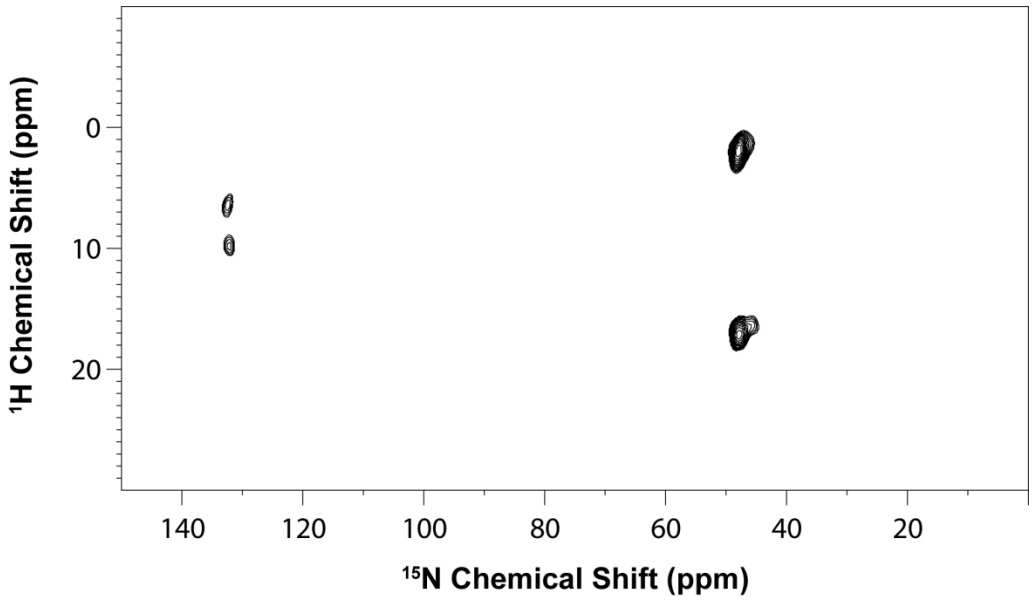

B-

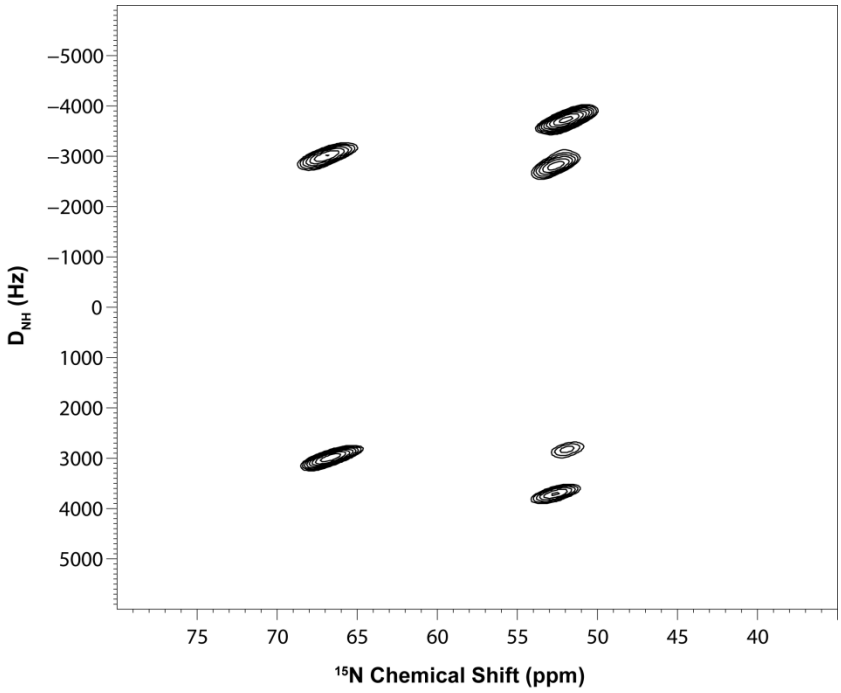

Figure S2. Spectra of ^{15}N-labeled T21G22 p1 and F6I9A12 p3 in 3:1 DMPC/DMPG collected at 313 K and using a peptide-to-lipid ratio of 1:20 (molar). A- 2-D de-HETCOR NMR spectrum of T21G22 p1. B) PISEMA spectrum of F6I9A12 p3. The dipolar dimension of the PISEMA spectrum was not adjusted for the scaling of 0.81 that results from using the Lee–Goldburg homonuclear decoupling sequence but Table S2 gives the corrected dipolar couplings.

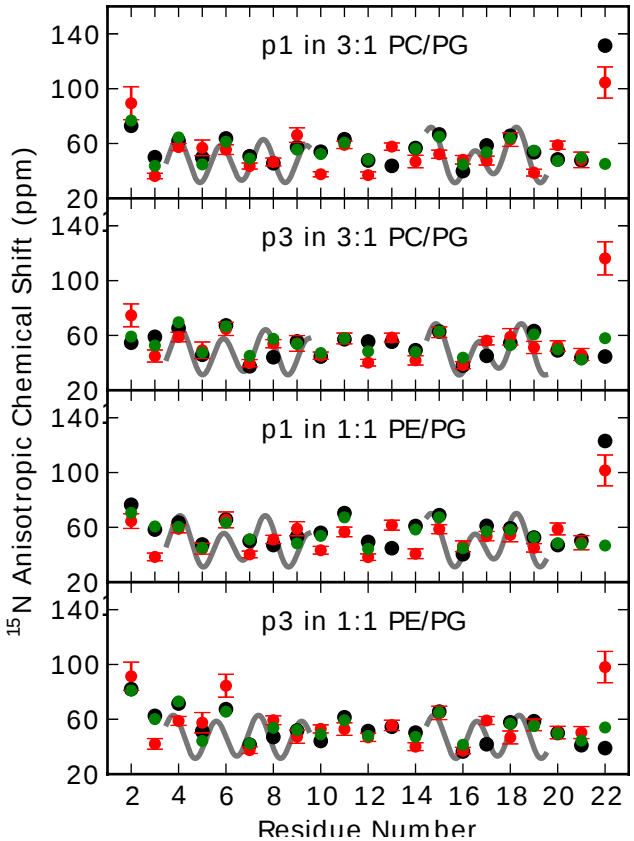

Figure S3. CSA restraints experimentally observed (black), calculated from the refined NMR structures (green), and calculated from the MD simulations (red): Piscidin 1 in 3:1 DMPC/DMPG (top) and 1:1 POPE/POPG (bottom-middle); Piscidin 3 in 3:1 DMPC/DMPG (top-middle) and 1:1 POPE/POPG (bottom). CS waves fitted to the experimentally observed CS values between residues 3-10 and residues 14-20 are shown in gray for an ideal α-helix with dihedral angles (ϕ=-61°, ψ=-45°).

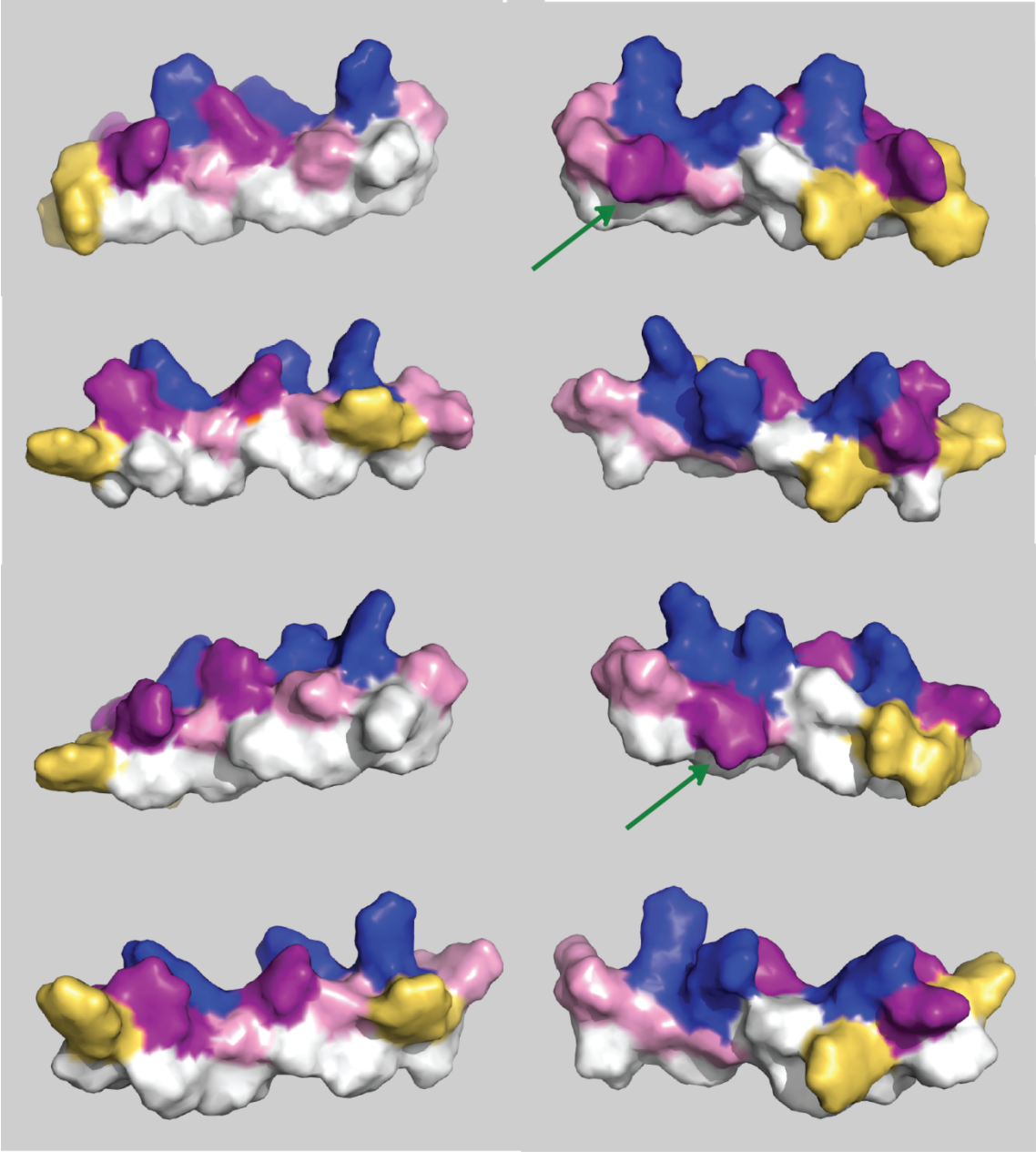

Figure S4. Surface charge of p1 and p3 in 3:1 PC/PG and 1:1 PE/PG. P1 is shown in PC/PG and PE/PG in the top and bottom-middle panels, respectively. P3 is shown in PC/PG and PE/PG in the top-middle and bottom panels, respectively. The left and right panels show the front (amino end on the left) and back views (amino end on the right) of each structure. Positively charged Arg and Lys are in blue; Phe in yellow; His in purple; Gly, Ser, Thr in pink; and Ile, Leu, and Val in white. H17 is indicated with a green arrow.

References

(1) Yang, J. T.; Wu, C. S.; Martinez, H. M. *Methods Enzymol.* **1986**, *130*, 208-269

(2) Fu, R.; Gordon, E. D.; Hibbard, D. J.; Cotten, M. *J. Am. Chem. Soc.* **2009**, *131*, 10830-10831

(3) Marassi, F. M.; Opella, S. J. *J. Magn. Reson.* **2000**, *144*, 150-155

(4) Mesleh, M. F.; Opella, S. J. *J. Magn. Reson.* **2003**, *163*, 288-299

(5) Tian, Y.; Schwieters, C. D.; Opella, S. J.; Marassi, F. M. *J. Magn. Reson.* **2012**, *214*, 42-50

(6) Levenberg, K. *Quart. Applied Math.* **1944**, *2*, 164-168

(7) Marquardt, D. *SIAM J. Appl. Math.* **1963**, *11*, 431-411

(8) Perrin Jr., B. S.; Pastor, R. W.; Cotten, M. In *Advances in Biological Solid-State NMR: Proteins and Membrane-Active Peptides*; Separovic, F., Naito, A., Eds.; Royal Society of Chemistry: Cambridge, 2014, p 18-35.

(9) Bertram, R.; Asbury, T.; Fabiola, F.; Quine, J. R.; Cross, T. A.; Chapman, M. S. *J. Magn. Reson.* **2003**, *163*, 300-309